CO12-1 Approach for Structural Analysis of Boundary Lubrication Film by Means of Neutron Reflectometry

T. Hirayama, Y. Konishi, M. Maeda, T. Matsuoka
M. Hino[1], M. Kitaguchi[1] and T. Oda[1]

Dept. of Mechanical Engineering, Doshisha University
[2]Research Reactor Institute, Kyoto University

INTRODUCTION: Boundary lubrication is one of the most interesting topics in the field of tribology, and the recent development of physical and chemical analyzers has been created a need for better understanding of the behavior of boundary lubrication films. Boundary lubrication films are classically divided into two principal categories; one is adsorbed layers due to physical or chemical bonding to a surface and the other is chemical reaction films, called 'tribofilm', formed in a friction process. The former is formed by natural adsorption of friction modifier (FM) additives, while the latter is formed due to chemical reaction between extreme pressure (EP) additives in lubricants and metal surfaces[1,2]. A better understanding of both behaviors is quite important and has been necessary in the field of tribology. However, analysis of the former is more difficult than that for the latter in general because the adsorbed additive layer is only nanometers thick, and should be *in-situ* analyzed under lubrication to prevent it from drying. Therefore, there has been still larger room for discussion in the former.

We have applied neutron reflectometry for structural analysis of boundary lubrication films under lubrication for several years. We found that the adsorbed layers on the metal surfaces were homogeneously formed by acetic acid and that the adsorbed layers on the iron and copper surfaces were quite thin, only 2 nm, with the almost half and same density as that of bulk acid, respectively.

For easier availability, we developed a TOF-mode neutron reflectometer for structural analysis of solid-liquid interface in the CN-3 in KURRI.

EXPERIMENTS: The beam path in the developed neutron reflectometer is illustrated in Fig. 1. White neuron beam passed through the chopper and two slits comes to sample, and the reflected beam goes to the detector through the detector slit. The detector can analyze the wave length of the reflected beam along the principle of time-of-flight (TOF).

SAMPLE: Nickel thin films on silicon wafers were prepared for first experiment. The Thickness of nickel films were 30 and 40 nm. The measurement was conducted in air, not in lubricant, first.

RESULTS: The obtained reflectivity profiles are shown in Fig. 2. We obtained the clear fringes from the nickel films. The theoretical fitting lines are also shown in the figure. We can see that the theoretical fitting lines on the assumption of 30 and 40 nm-thickness agree with each experimental profile. We concluded that the resolution of the developed reflectometer is approximately 1 nm and that the reflectometer promises to be useful for structural analysis at the sample surface or interface.

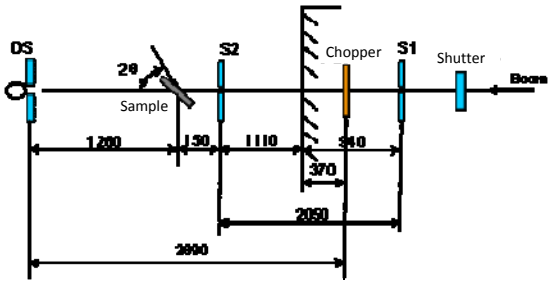

Fig. 1. Beam path in the developed neutron reflectometer in CN-3 in KURRI.

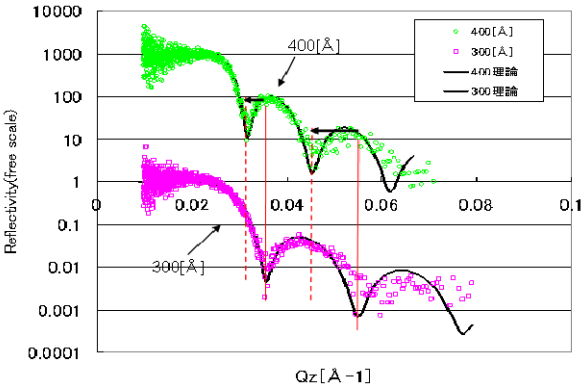

Fig. 2. Reflectivity profiles of nickel films with various thickness on silicon wafers.

REFERENCES:

[1] Hutchings, I.M., Tribology - Friction and Wear of Engineering Materials, 1992, Arnold, London.
[2] Hardy, W.B. and Bircumshaw, I., Boundary Lubrication - Plane Surfaces and the Limitations of Amontons' Law, Proc. R. Soc. Lond., A108 (1925) 1-27

採択課題番号 22030　　中性子反射率法による表面吸着層構造解明へのアプローチ　　共同通常
（同志社大・理工）平山朋子、小西庸平、前田成志、松岡敬（京大・原子炉）日野正裕、北口雅暁、小田達郎

CO12-2 Specification of Arsenic in Seaweeds

M. Fukushima[1], S. Fukutani[2] and Y. Nakano[2]

[1]*Department of Basic Sciences, Ishinomaki Senshu University*
[2] *Research Reactor Institute, Kyoto University*

INTRODUCTION: Hijiki is one of edible seaweeds and popular for Japanese people. Also hijiki has an important role of iodine source in Japanese daily foods. At the same time, it is known that hijiki contains rather high levels of Arsenic (As). For estimating As level in cooked hijiki, we have analyzed several different hijiki samples by ICP-AES. Also the results were compared with those obtained by neutron activation analysis (NAA).

EXPERIMENTALS: Samples: Generally, raw hijiki is collected from shallow shores in early February to May, steamed in the net in western Japan or boiled in steamer in eastern Japan. Then the heated hijiki is dried, packed in a bag, and sold in the market. In this work, we have collected raw hijiki in Onagawa Bay, Ishinomaki, in April. Then the raw hijiki was boiled in a beaker with or without iron marble for modifying the boiling method at locations in eastern or western Japan. After boiling for 3 or 6 hours, hijiki was freeze-dried. For comparison, dried hijiki from Ishinomaki in Miyagi, Enoshima in Kanagawa and Nagasaki in Nagasaki, was bought in the market. All of the dried hijiki was pulverized by mill.

Cooking of hijiki: Boiled and dried hijiki was soaked in tap water overnight, then wet hijiki was cooked with the mixture of water, soy sauce, sugar, Japanese sake, and powdered broth in the same way as we do in the kitchen. Cooked hijiki was freeze-dried and pulverized.

Analysis of As by ICP-AES: Approximately 0.5 g of dried powder was digested by nitric acid, and filtered through a 0.45 μm membrane filter. NIST SRM 1566b Oyster Tissue was digested in a same way as hijiki.

Analysis of As by NAA: Another portion of dried sample was irradiated in KUR for analyzing As. Approximately 0.3 g of sample was sealed in a polyethylene sheet, irradiated in KUR for 1 hour by 1 MW, and gamma rays were measured after 1week cooling time.

RESULTS: Levels of As and Fe in hijiki after several different treatments are shown in Table 1. From Table 1, As levels in hijiki after boiling decreated comparing to control (no treatment). On the contrary, As level did not change much after steaming raw hijiki. This indicates boiling raw hijiki with water has a reducing effect of As in hijiki. As for Fe, Fe level in hijiki boiling with iron marble in the water markedly increased compared to the control. And the levels increased by boiling for a longer time. As and Fe levels in dried hijiki on the market are shown in Table 2.

From the results shown in Table 2, the Fe level in Nagasaki hijiki was low compared to Miyagi and Enoshima hijiki, and it indicates the difference of treatment method. When the results were obtained by ICP-AES and NAA, values were not different for the same sample. However the Fe value in Miyagi hijiki (2009) showed a noticeable difference between ICP-AES and NAA results. Seaweeds contain high levels of polysaccharides, Na, K and some other elements, which have an interfering effect with other trace elements in many analytical methods. These obstructions are thought to remain considerably in the solution after acid digestion. Also, we have to think about the possibility of loss of elements by filtering of sample solutions before analyzing with ICP-AES. ICP-AES is a powerful tool for analyzing multi-elements simultaneously. We should pay attention to analyze solution which have complex matrix such as seaweed samples. As and Fe levels in cooked hijiki are shown in Table 3.

By comparing Table 2 and 3, it is clear that As levels decreased to approximately 20 ppm by the cooking process. On the contrary, Fe levels did not decrease markedly.

From this work, we knew that main source of Fe in cooked hijiki (eastern Japan) came from the cooking instrument (i.e., steamer).

ACKNOWLEDGEMENT: We would like to thank to Dr. Takenari Matsutani in Ishinomaki Senshu University and Mr. Abe for collection of hijiki.

Table 1. As and Fe levels after the treatment of raw hijiki.

Treatment for hijiki		As (ppm)*	Fe (ppm)*
control		90	26
steam		81	43
Boiling time (hr)	Iron marble		
3	without	39	32
3	with	54	923
6	without	54	39
6	with	43	1510

* concentration is calculated by dry weight base

Table 2. As and Fe levels in dried hijiki from different producers.

hijiki producer	As (ppm)*		Fe (ppm)*	
	ICP-AES	NAA	ICP-AES	NAA
Miyagi (2009)	57	54	558	816
Miyagi (2010)	20	29	676	706
Enoshima	128	132	201	224
Nagasaki	113	138	53	80

* concentration is calculated by dry weight base

Table 3. As and Fe levels of hijiki after cooking.

cooked hijiki	As (ppm)*		Fe (ppm)*	
	ICP-AES	NAA	ICP-AES	NAA
Miyagi (2009)	20	8	405	368
Enoshima	22	15	135	126
Nagasaki	22	19	44	48
Onagawa (steamed)	17	13	30	40

* concentration is calculated by dry weight base

採択課題番号 22044 海草に含まれるヒ素の化学種同定 共同通常
（石専大・理工）福島美智子、吉原 章（京大・原子炉）福谷 哲、中野幸廣

CO12-3 Effect of Co-cultured Silicon Particles on Neural Stem Cell

K. Fujioka, N. Fujii[1], K. Sato[2], K. Hirakuri[3], S.U. Kim[4], and Y. Manome[1]

Institute of DNA Medicine, Jikei University School of Medicine
[1]*Research Reactor Institute, Kyoto University*
[2]*Department of Physics, University of Bologna*
[3]*Department of Electrical and Electronic Engineering, Tokyo Denki University*
[4]*Department of Medicine, University of British Columbia*

INTRODUCTION: Semiconductor quantum dots (QDs) are nanoparticles and exhibit brighter and longer fluorescence than organic dyes. Taking advantage of these characteristics, QDs are utilized as fluorescent labels in many biological studies.

Fluorescent silicon QDs (synthesized in Tokyo Denki University) have ability of cell labeling and lower toxicological effect for HeLa cells in mitochondrial activity assay [1]. In this assay, the silicon QDs affected the cells over a concentration of 1 mg/mL due to their slight radical productivity. Radical productivity was also known in titan dioxide particles.

Recent studies suggested that free radicals cause some health problems such as Alzheimer's disease. In this study, we investigate the effect of the silicon QDs on the activity of human neural stem cells.

EXPERIMENTS: The silicon QDs were prepared by the spattering and passive oxidization method in our previous report [1, 2]. The immortalized human neural stem cell line was established by Kim et al. [3].

The neural stem cells (1×10^4 cells/mL) were cultured in DMEM containing 10% FCS for 48 hours. Then the cells were co-cultured with the indicated concentration of silicon QDs for 48 hours. After the co-culture, mitochondrial activity was measured with Cell Counting Kit-8 (Dojindo). Quantities of cytokines and chemokine in the co-cultured medium were measured with Multi-Analyte ELISArray^{TM} Kit (Human Autoimmune Response; SA-Biosciences). This kit analyzes a panel of 12 cytokines and chemokines (IL-1B, IL-4, IL-6, IL-10, IL-12, IL-17A, IFN-γ, TNF-α, TGF-β1, MCP-1, MIP-1α, and MIP-1β).

For the detection of D-β-amino acid formation, the co-cultured cells (0, 1 and 100 μg/mL) were lysed with M-PER Mammalian Protein Extraction Reagent (Pierce). After the separation on 5% SDS-PAGE gel, the gel was transferred to PVDF membrane. The membrane was reacted with anti-D-β-Asp polyclonal antibody [4].

RESULTS: As shown in Fig. 1 (A), mitochondrial activity of the human neural stem cell line had an increasing tendency depending on the concentration of the silicon QDs. This tendency indicates the cellular proliferation between the concentrations of 1-100 μg/mL. Next, we investigated the cytokines and chemokines of the co-cultured medium for revealing the mechanism of the proliferation. Among the investigated cytokines and chemikines, IL-6 increased in the co-cultured medium (Fig. 1 (B)). IL-6 has pleiotropic function such as inflammatory mediator, growth factor, and bone resorption factor. This cytokines may cause proliferation and differentiation.

In order to investigate D-β-amino acid formation by silicon QDs, the co-cultured cell lysates (6 μg of total protein) were loaded and reacted with anti-D-β-Asp antibody. At the concentration of the protein, we could not detect the D-β-amino acid (data not shown).

In conclusion, the human neural stem cell line showed proliferation tendency and IL-6 release under the co-cultured condition. In the future study, we should reveal the cytokine releasing mechanisms and the cellular differentiation.

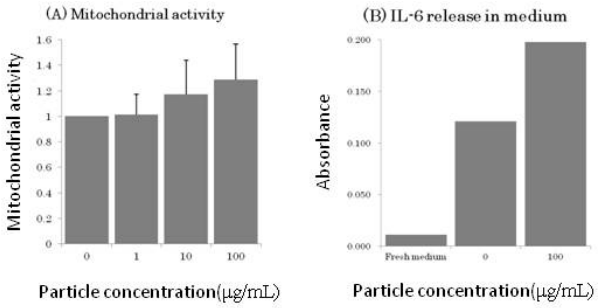

Fig. 1. The effect of silicon QDs on the activity of human neural stem cells. Mitochondrial activity of the cells (A) and IL-6 in the co-cultured medium (B).

REFERENCES:

[1] K. Fujioka *et al.*, Nanotechnology, **19** (2008) 415102(7pp).
[2] K. Shinoda *et al.*, J. Cryst. Growth, **288** (2006) 84-86.
[3] S. U. Kim *et al.*, Neuropathology, **24** (2004) 159-171.
[4] N. Fujii *et al.,* Mol. Vis. **6** (2000) 1-5.

CO12-4 Mössbauer Spectra Measurements of Synthetic and Natural Magnetites

K. Shinoda, C. Tomita, T. Taniguchi and Y. Kobayashi[1]

Department of Geosciences,
Graduate School of Science, Osaka City University
[1]Research Reactor Institute, Kyoto University

INTRODUCTION: Magnetite is a typical Fe-oxide mineral. The crystal structure of magnetite is inverse spinel type. Chemical compositions of magnetite vary from $[Fe^{3+}]^A[Fe^{3+}, Fe^{2+}]^BO_4$ to $[Fe^{3+}]^A[Fe^{3+}_{5/3}, x_{1/3}]^BO_4$, where x indicates vacancy in B site. Since the vacancy is controlled by oxygen fugacity, quantitative analyses of vacancy of natural magnetite are of interest to estimate regional environments. Crystallographic ways to measure vacancies of magnetite are X-ray diffraction analyses and Mössbauer spectra measurements. In this study, vacancies of synthetic and natural magnetite are estimated from X-ray and Mössbauer analyses, and the relationships of vacancies estimated from the two independent ways are evaluated.

EXPERIMENTS: Seven vacancy-variant magnetite are synthesized from synthetic powdered magnetite. The synthetic magnetite are made by reducing powdered reagent of hematite. Natural maganetites were collected from five different occurrences. Chemical compositions of natural magnetite were measured using SEM-EDS. TiO_2 and Al_2O_3 were detected as solid solution components. Mössbauer spectra of synthetic and natural magnetite were measured at Seto Lab. Powdered magnetite of 10mg were mixed well with powdered agarose of 100mg and pressed into a pellet. The pellet was exposed to γ-ray generated from ^{57}Co for 24 hours. By fitting the measured spectra by Lorentz function, peak area due to Fe in A and B sites are calculated. Vacancy ratio was estimated from the ratio of peak area of A and B sites [1]. In the estimation of vacancies of natural magnetite, which often contain TiO_2, it was assumed that the ulvöspinel component do not contribute to the magnetic splitting.

RESULTS: Figure 1 indicates a liner relation of vacancy estimated by two independent methods. This suggests that vacancies of magnetite free from TiO_2 can be estimated by both Mössbauer and X-ray methods. Natural magnetite generally contains TiO_2 and makes solid solution with ulvöspinel Fe_2TiO_4. As no magnetic splitting is observed in ulvöspinel, we subtracted ulvöspinel componet from the natural magnetite, and estimated vacancy by fitting Mössbauer spectra into the remaining component. But as shown in Fig.2, clear gap was observed in vacancies estimated by two independent methods. It should be required to establish a way to estimate vacancy of titanomagnetite.

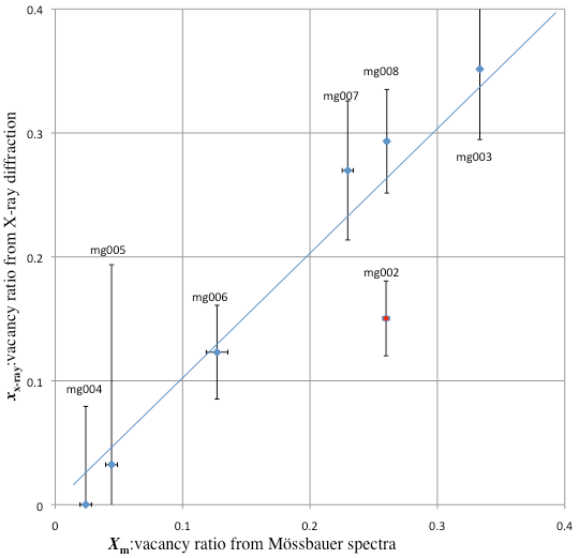

Fig. 1. Vacancy ratio of synthetic magnetite estimated from Mössbauer spectra and X-ray diffraction.

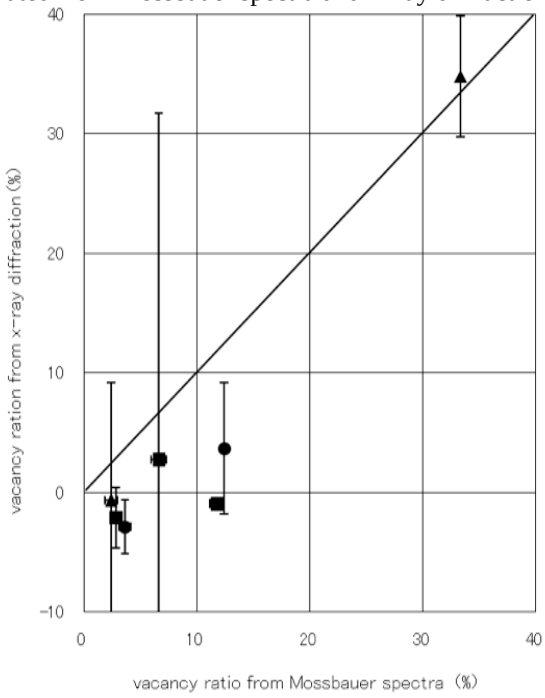

Fig. 2. Vacancy ratio of natural magnetite estimated from Mössbauer spectra and X-ray diffraction. Circles are from sand, squares are in rock, triangles are synthetic.

REFERENCES:

[1] K. Volenik, M Seberini, J. Neid Czech. J. Physics **25** (1975) 1063-1071.

採択課題番号 22066　　マグネタイト−マグヘマイト系鉄酸化鉱物の　　共同通常
メスバウアースペクトル測定
（大阪市大・理）篠田圭司、富田千尋、谷口隆文　（京大・原子炉）小林康浩